

## Eisvogel: Exact and efficient calculations of radio emissions from in-ice neutrino showers

---

Philipp Windischhofer,<sup>a,\*</sup> Christoph Welling<sup>b</sup> and Cosmin Deaconu<sup>b</sup>

<sup>a</sup>University of Chicago, Enrico Fermi Institute, Chicago, IL 60637

<sup>b</sup>University of Chicago, Astronomy & Astrophysics, Kavli Institute for Cosmological Physics, Chicago, IL 60637

E-mail: [philipp.windischhofer@uchicago.edu](mailto:philipp.windischhofer@uchicago.edu), [christophwelling@uchicago.edu](mailto:christophwelling@uchicago.edu), [cozzyd@kicp.uchicago.edu](mailto:cozzyd@kicp.uchicago.edu)

The detection of the radio signature of in-ice charged-particle showers is a promising technique for the study of ultra-high-energy neutrinos. Planned large-scale radio arrays require a thorough understanding of the generation and propagation of electromagnetic radiation in the heterogeneous environment of polar ice. In this contribution, we introduce Eisvogel, a simulation tool for the first-principles calculation of the time-domain signal observed by an antenna in such an experiment. Eisvogel calculates the exact antenna signal through the numerical convolution of the shower with a precomputed Green's function that encodes the properties of the surrounding ice and the antenna and captures all electrodynamic effects. Numerically expensive calculations are thus amortized into the construction of the Green's function, with the signal calculation for a given shower remaining very efficient. Here, we describe the structure of our code and the current stage of development, show a comparison with an established simulator, and outline future applications.

38th International Cosmic Ray Conference (ICRC2023)  
26 July - 3 August, 2023  
Nagoya, Japan



---

\*Speaker

## 1. Introduction

Experiments that aim to detect ultra-high energy cosmic neutrinos through the radio emissions of charged-particle cascades developing in glacial ice require a thorough understanding of the creation, propagation, and detection of electromagnetic waves in this complex environment. This necessitates the accurate modelling of all relevant material properties, summarized in a position-dependent, anisotropic index of refraction as well as the reception characteristics of each antenna station.

To ensure a computationally efficient implementation, currently existing simulation codes typically work in the approximation of geometric optics, where the propagation of electromagnetic radiation through the ice environment is performed with ray tracing [1]. However, realistic ice geometries may involve feature sizes that are of the order of the targeted wavelengths and can thus support phenomena that lie outside the realm of geometric optics. These include, for example, surface radiation modes [2] that propagate along the ice-air interface, or the presence of thin reflective subsurface features [3].

Accurately simulating these effects entails, in principle, solving Maxwell's equations over the entire instrumented ice volume, where the signal-generating charged-particle shower is included as a source current distribution  $\mathbf{J}(\mathbf{x}, t)$ , and the environment is represented by a position- and frequency-dependent distribution of permittivity  $\hat{\epsilon}(\mathbf{x}, \omega)$ , permeability  $\hat{\mu}(\mathbf{x}, \omega)$ , and conductivity  $\hat{\sigma}(\mathbf{x}, \omega)$ . These material parameters are generally matrix-valued, reflecting the anisotropic nature of the ice.

The shower may have an arbitrary orientation with respect to the ice surface and the antenna. The absence of any symmetries mandates a fully three-dimensional calculation, and the extreme scale ratio between the domain of interest (with a linear length of  $\mathcal{O}(\text{km})$ ) and the targeted wavelength ( $\mathcal{O}(\text{cm})$ ) for waves in the frequency range of interest of 100 MHz–1 GHz renders this approach infeasible in practice.

In this contribution, we present the simulation code *Eisvogel* [4], currently under development, which is designed to compute the exact antenna signal for a given shower current distribution in an extremely efficient manner. All electrodynamic effects are automatically included in the simulation without requiring to solve Maxwell's equations anew for each considered shower. *Eisvogel* makes this possible by first constructing an electrodynamic Green's function for the signal delivered by an antenna. This expensive operation needs to be performed only once for each antenna and environment specification. The antenna signal for a given event is then obtained through an efficient numerical convolution of the Green's function with the shower.

This document is organized as follows. Section 2 gives a high-level overview of the theoretical background and the structure of the *Eisvogel* code. The current state of development and simulation results for a representative situation are presented in Section 3. Section 4 summarizes potential applications of the code.

## 2. Overview of the code

Fig. 1 shows a graphical representation of the signal simulation as implemented in *Eisvogel*. The code handles the construction of an electrodynamic Green's function  $\mathbf{K}(\mathbf{x}, t)$  for a specific antenna

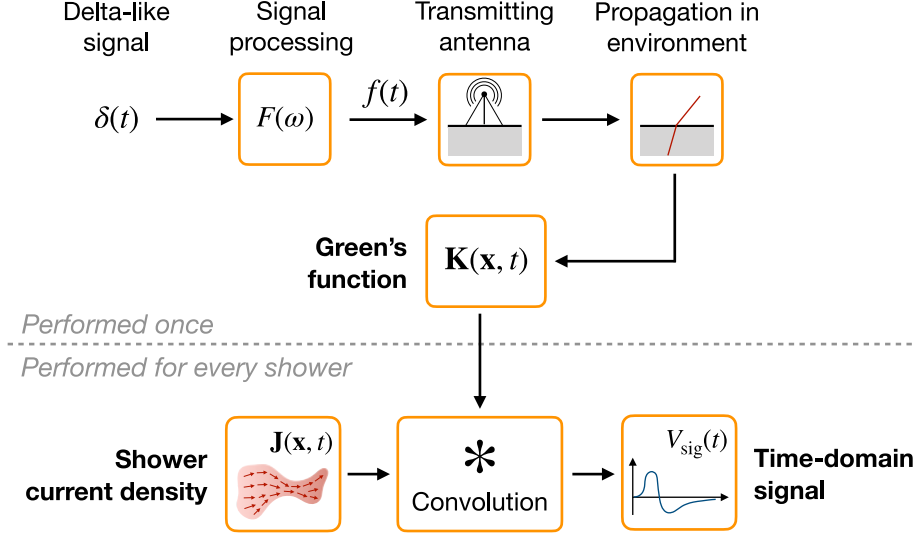


**Figure 1:** Structure of the *Eisvogel* simulation code, including the calculation of the electrodynamic Green’s function  $\mathbf{K}(\mathbf{x}, t)$  (top half) and the computation of the induced signal through its convolution with the current density  $\mathbf{J}(\mathbf{x}, t)$  of the charged-particle cascade (bottom half).

configuration and environment, as well as the application of this Green’s function to a given current distribution  $\mathbf{J}(\mathbf{x}, t)$  to compute the time-domain antenna signal  $V_{\text{sig}}(t)$ . The latter may be expressed through a convolution integral of the form [5, 6]

$$V_{\text{sig}}(t) = - \int d^3\mathbf{x}' dt' \mathbf{K}(\mathbf{x}', t - t') \cdot \mathbf{J}(\mathbf{x}', t'). \quad (1)$$

(The overall minus sign in this expression is of no physical relevance and chosen by convention.)

The conceptual foundations of both steps are briefly discussed in the following. An in-depth description of the implementation in *Eisvogel* is the subject of a forthcoming publication.

## 2.1 Calculation of the Green’s Function

In a radio neutrino experiment, the raw time-domain voltage waveform delivered by an antenna is further processed and filtered by its front-end electronics. This filtering operation is assumed to be a linear operation that may be represented in the frequency domain by a transfer function  $F(\omega)$  or by the corresponding impulse response  $f(t)$  in the time domain. The filtered signal  $V_{\text{sig}}(t)$  is then used for the reconstruction of the shower-initiating neutrino and, as such, is the quantity that one wishes to simulate.

As explained in Refs. [5, 6], it is possible to construct a Green’s function for  $V_{\text{sig}}(t)$  by propagating a delta-like signal through the full signal path in reverse. As shown in Fig. 1, the Green’s function  $\mathbf{K}(\mathbf{x}, t)$  is the electric field distribution radiated by the antenna if a current  $I(t) \sim f(t)$  is applied to its terminals. This is a well-defined electrodynamics problem that may be solved numerically for arbitrary material geometries ( $\hat{\epsilon}(\mathbf{x}, \omega)$ ,  $\hat{\mu}(\mathbf{x}, \omega)$ ,  $\hat{\sigma}(\mathbf{x}, \omega)$ ).

Before considering this general case, it is useful to study the much simpler situation of an electric dipole antenna embedded in a homogeneous and isotropic material, for which the Green’s function exists analytically. For a dipole oriented along the  $z$ -axis in a medium with permittivity  $\epsilon$

and vanishing conductivity  $\sigma \equiv 0$ , it reads (in spherical coordinates),

$$K_r(r, \theta) = -2 \frac{L}{4\pi\epsilon} \frac{\cos \theta}{r^3} \left[ f_0 \left( t - \frac{rn}{c} \right) + \frac{rn}{c} f \left( t - \frac{rn}{c} \right) \right], \quad (2)$$

$$K_\theta(r, \theta) = -\frac{L}{4\pi\epsilon} \frac{\sin \theta}{r^3} \left[ f_0 \left( t - \frac{rn}{c} \right) + \frac{rn}{c} f \left( t - \frac{rn}{c} \right) + \left( \frac{rn}{c} \right)^2 f' \left( t - \frac{rn}{c} \right) \right], \quad (3)$$

$$K_\varphi(r, \theta) = 0, \quad (4)$$

provided that the effective length  $L$  of the antenna is small compared to the wavelengths of interest. In Eqs. 2–4,  $r$  and  $\theta$  are the radial coordinate and polar angle, respectively,  $\varphi$  is the azimuthal angle,  $n$  is the index of refraction of the medium, and  $c$  is the speed of light in vacuum. The Green's function contains the expressions  $f'(t)$  and  $f_0(t)$ , which are related to the impulse response  $f(t)$  of the signal processing chain,  $f'(t) = df/dt$  and  $f_0(t) = \int_{-\infty}^t dt' f(t')$ . For most situations, these functions are smooth, well-behaved expressions. For example, in the practically relevant case where the signal-processing chain implements a low-pass filter of order  $N$  and peaking time  $t_p$ , we have

$$F(\omega) = \frac{1}{(1 + i\omega t_p/N)^{N+1}}, \quad f(t) = \frac{1}{t_p(N-1)!} \left( \frac{Nt}{t_p} \right)^N e^{-Nt/t_p}. \quad (5)$$

For fully general material distributions and antenna characteristics, Eisvogel interfaces to the finite-difference time-domain (FDTD) code Meep [7] to solve Maxwell's equations and find the Green's function. While still nontrivial, symmetries often considerably reduce the computational effort required to construct a Green's function. For example, in the common case where the reception characteristic of the antenna and the surrounding environment are (approximately) cylindrically symmetric, also the Green's function inherits this (approximate) symmetry. It can then be parameterized by the vertical coordinate  $z$  and the radius  $r_{xy}$  in the  $xy$ -plane, reducing to a two-dimensional electrodynamics problem which is significantly easier to solve numerically. Furthermore, it is often possible to separate the environment into a domain where the material parameters are strongly position-dependent, and a surrounding homogeneous “exterior” region of much larger spatial extent. For example, the complicated geometry of the firm ice is sandwiched between the much more homogeneous bulk ice on one side and the atmosphere on the other side. In such situations, it is possible to restrict the FDTD calculation to the spatially inhomogeneous region, impose transparent boundary conditions, and then extend the resulting Green's function to the exterior domain by manually propagating the outgoing radiation field through the Rayleigh-Sommerfeld diffraction integral [8]. Taken together, this technical infrastructure allows in-situ measurements of the ice geometry to be directly taken into account in the Green's function from first principles.

To illustrate these aspects, Fig. 2 shows the Green's function computed with Meep for a dipole antenna located in a simple material geometry representative of an in-ice neutrino observatory. Similar to the analytic solution in Eqs. 2–4, it shows wavefronts that propagate away from the antenna at the local phase velocity. Moreover, the Green's function exhibits genuine wave-optics phenomena, such as propagating surface modes, which were already identified in the previous simulation study of Ref. [9].

## 2.2 Sampling, interpolation, and convolution

The Green's function  $\mathbf{K}$  derived for a given geometry must be kept in non-volatile memory from which it may be retrieved and used for the calculation of the antenna signal at a later time. As

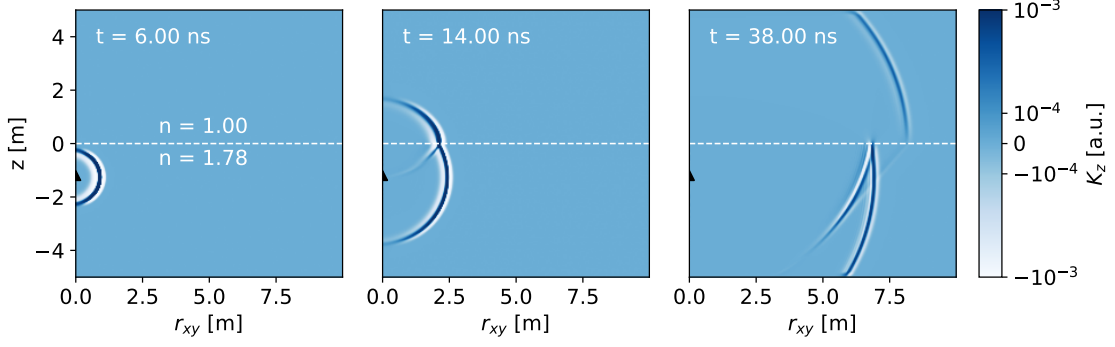


**Figure 2:** The vertical component  $K_z$  of the Green's function for a vertically oriented infinitesimal electric dipole antenna (marked by the black triangle), computed with Meep [7]. The antenna is embedded in a material geometry with  $n = 1$  for  $z > 0$  and  $n = 1.78$  for  $z < 0$ ; the transition between both components is marked by the white dashed line. A low-pass filter of the form of Eq. 5 with  $N = 6$  and  $t_p = 1$  ns is used. The field is displayed in cylindrical coordinates, where  $z$  labels the vertical direction and  $r_{xy}$  is the radial distance measured in the  $xy$ -plane.

discussed above, the Green's function represents the electromagnetic radiation pattern resulting from a band-limited current source and is thus itself band-limited in space and in time. It can therefore be represented without loss of information by a collection of regularly spaced samples taken at positions  $(\mathbf{x}_i, t_j)$ , so long as the sampling frequency in each coordinate direction is not smaller than the respective Nyquist frequency. The Green's function may be evaluated at an arbitrary intermediate location  $(\mathbf{x}, t)$  by interpolating between the samples  $\mathbf{K}(\mathbf{x}_i, t_j)$ . The interpolation is a linear operation that combines neighbouring sample values through the interpolation kernel  $h$ ,

$$\mathbf{K}(\mathbf{x}, t) = \sum_{i,j} h(\mathbf{x} - \mathbf{x}_i, t - t_j) \mathbf{K}(\mathbf{x}_i, t_j). \quad (6)$$

The explicit form of Eq. 6 depends on the coordinate system in which the Green's function is expressed. In cartesian coordinates, the voxel specified by the vector index  $\mathbf{i} = (i_x, i_y, i_z)$  and the temporal index  $j$  is centered on the position  $\mathbf{x}_i = (\Delta x \cdot i_x, \Delta y \cdot i_y, \Delta z \cdot i_z)$  and the time  $t_j = \Delta t \cdot j$ . The intervals  $\Delta x$ ,  $\Delta y$ ,  $\Delta z$ , and  $\Delta t$  are the respective sampling intervals. Eq. 6 may then be written as the product of the interpolation kernels  $h_1$  for the respective coordinate directions

$$h(\mathbf{x} - \mathbf{x}_i, t - t_j) = h_1\left(\frac{x}{\Delta x} - i_x\right) h_1\left(\frac{y}{\Delta y} - i_y\right) h_1\left(\frac{z}{\Delta z} - i_z\right) h_1\left(\frac{t}{\Delta t} - j\right).$$

Linear interpolation corresponds to  $h_1(n) = (1 - |n|) H(1 - |n|)$  with the Heaviside step function  $H$ . By default, Eisvogel uses the cubic interpolation kernel derived in Ref. [10], which guarantees that the interpolation error decreases with the third power of the sampling interval. In cases where the Green's function has cylindrical symmetry, an equidistant grid in polar coordinates is used. The spatial interpolation in Eq. 6 then involves summing over  $\mathbf{i} = (i_{r_{xy}}, i_z)$  with  $\mathbf{x}_i = (\Delta r_{xy} \cdot i_{r_{xy}}, \Delta z \cdot i_z)$ .

Like the Green's function, also the source current density  $\mathbf{J}(\mathbf{x}, t)$  is taken to be band-limited and thus subject to an interpolation relation similar to Eq. 6. Note that the current samples  $\mathbf{J}(\mathbf{x}_i, t_j)$  need not necessarily be specified on the same grid as those of the Green's function. It is useful, for example, to align one of the coordinate axes with the propagation direction of the shower. This

coordinate system is then generally rotated with respect to the antenna coordinate system. For simplicity, we will nevertheless continue to use the same notation for samples specified in either coordinate system.

Given the two sets of samples  $\mathbf{K}(\mathbf{x}_i, t_j)$  and  $\mathbf{J}(\mathbf{x}_i, t_j)$ , their convolution is then performed as follows. First, the Green's function and the current density are interpolated onto a common grid so that the product  $\mathbf{K}(\mathbf{x}', t - t') \cdot \mathbf{J}(\mathbf{x}', t')$  appearing in the integrand of Eq. 1 may be evaluated. In terms of the integration variables  $\mathbf{x}'$  and  $t'$  the integrand then takes the form

$$\mathbf{K}(\mathbf{x}', t - t') \cdot \mathbf{J}(\mathbf{x}', t') = \sum_{i,j} h(\mathbf{x}' - \mathbf{x}'_i, t' - t'_j) \mathbf{K}(\mathbf{x}'_i, t - t'_j) \cdot \mathbf{J}(\mathbf{x}'_i, t'_j).$$

Integrating the above expression and using the fact that the one-dimensional interpolation kernel must integrate to unity,  $\int dn h_1(n) = 1$ , Eq. 1 may be written as

$$V_{\text{sig}}(t) = - \int d^3\mathbf{x}' dt' \mathbf{K}(\mathbf{x}', t - t') \cdot \mathbf{J}(\mathbf{x}', t') = -\Delta V \sum_{i,j} \mathbf{K}(\mathbf{x}'_i, t - t'_j) \cdot \mathbf{J}(\mathbf{x}'_i, t'_j), \quad (7)$$

with the voxel volume  $\Delta V = \Delta x \Delta y \Delta z \Delta t$ . The convolution integral in the form of Eq. 7 is well-suited for an efficient vectorized evaluation.

### 3. Comparison with ARZ

To illustrate the utility of this approach, we use it to compute the signal produced by an exemplary electromagnetic shower, parameterized by the longitudinal charge excess profile taken from the publicly available library of Ref. [11]. The shower energy is 1 EeV. The evolution of the charge excess, visualized in Fig. 3a, is affected by the Landau-Pomeranchuk-Migdal (LPM) effect. The transverse extent of the shower is not parameterized.

The shower develops in a homogeneous and isotropic medium with an index of refraction of  $n = 1.78$  and is observed by an electric dipole antenna oriented along the vertical direction, positioned close to the Cherenkov cone. The signal is processed by a low-pass filter of the type of Eq. 5 with  $N = 6$  and  $t_p = 1$  ns, corresponding to a 3 dB-bandwidth of around 300 MHz.

Figs. 3b and 3c show simulation results for the antenna signal in the time- and frequency domain, respectively, as computed with Eisvogel and the ARZ algorithm [12] implemented in NuRadioMC [1]. To facilitate a comparison of the signal *shapes*, the simulated signals are normalized to their respective maximum values,  $V_{\text{sig}}(t)/V_{\text{sig}}^{\text{max}}$ . The results from both codes are in excellent agreement.

Note that, although the same one-dimensional shower profiles were passed as input to the two simulation codes, the resulting absolute signal amplitudes for this example situation cannot be directly compared, and are thus not shown. This is due to differences in the internal treatment of the transverse charge profile between Eisvogel and ARZ: while the ARZ code in NuRadioMC automatically attempts to include the effect of the transverse shower profile through hard-coded form factors [12, 13], Eisvogel calculates and returns the signal produced by the specified one-dimensional shower current. The two approaches differ in the degree of coherence of the radio emission from different parts of the shower, and thus result in different absolute signal amplitudes.

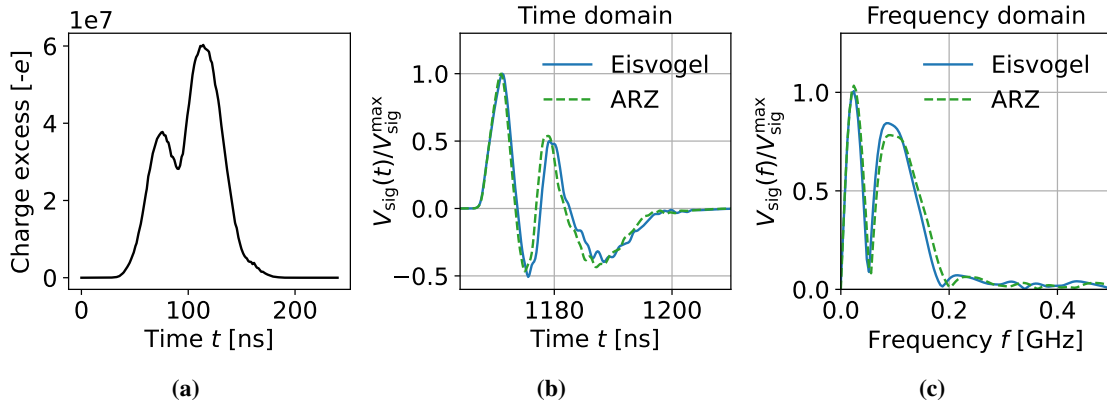


**Figure 3:** Simulation results for an electromagnetic shower with an energy of  $E = 10^{18}$  eV observed by a vertically-oriented dipole antenna placed at an angle of  $\phi - \phi_c = 1^\circ$  with respect to the Cherenkov cone. (a) Excess charge profile of the shower as a function of time in units of the electron charge. (b) Time-domain voltage signal delivered by the antenna, normalized to its maximum value. (c) Frequency-domain voltage signal delivered by the antenna, normalized to its maximum value. The solid blue curves show the signal as calculated by Eisvogel starting from a one-dimensional representation of the shower. The dashed green curves are calculated by the ARZ algorithm [12] implemented in NuRadioMC [1].

#### 4. Conclusions and outlook

In this contribution we have introduced Eisvogel, a numerical code for the efficient calculation of neutrino-induced antenna signals in complicated environments such as those faced by in-ice radio neutrino observatories or balloon experiments. The central element of the code is an electrodynamic Green’s function for the antenna signal, which contains information about the environment through which the radiation propagates, and allows the signal to be calculated starting from the shower current distribution. For the first time, this scheme makes the exact signal accessible in a numerically efficient manner, obviating the need for further approximations or simplifications that are commonly made in existing simulators.

These new capabilities have the potential to significantly improve the understanding of current and future experiments targeting ultra-high energy cosmic neutrinos or charged cosmic rays. For example, important instrumental backgrounds such as downgoing air showers that impact the ice from above can be simulated in a rigorous fashion, and their impact on the physics potential can be quantified. Propagation effects resulting from birefringence or impurities trapped in the ice are naturally and straightforwardly included in the signal simulation, allowing the region of validity of currently existing codes (and their corresponding approximations and assumptions) to be validated. This could be of relevance also for signals induced by air showers in cases where interactions of the radiation field with the environment are important, e.g. for highly-inclined showers observed by antennas positioned in mountainous terrain.

## References

- [1] C. Glaser et al., “NuRadioMC: Simulating the radio emission of neutrinos from interaction to detector”, EPJC 80, 77 (2020)
- [2] S. W. Barwick et al., “Observation of classically ‘forbidden’ electromagnetic wave propagation and implications for neutrino detection.”, JCAP07, 055, (2018)
- [3] I. M. Shoemaker et al., “Reflections on the anomalous ANITA events: the Antarctic subsurface as a possible explanation”, Annals of Glaciology, 61, 92–98 (2020)
- [4] P. Windischhofer, C. Welling, C. Deaconu, *Eisvogel* code repository, <https://github.com/philippwindischhofer/Eisvogel> (visited on 20/06/2023)
- [5] P. Windischhofer, W. Riegler, “Electrical signals induced in detectors by cosmic rays: a reciprocal look at electrodynamics”, PoS(ICRC2021), 184 (2021)
- [6] W. Riegler, P. Windischhofer, “Signals induced on electrodes by moving charges, a general theorem for Maxwell’s equations based on Lorentz-reciprocity”, Nucl. Instrum. Meth. A, 980, 164471 (2020)
- [7] A. F. Oskooi, D. Roundy, M. Ibanescu, P. Bermel, J. D. Joannopoulos, S. G. Johnson, “Meep: A flexible free-software package for electromagnetic simulations by the FDTD method”, Comput. Phys. Commun. 181, 687–702 (2010)
- [8] L. Zschiedrich, F. Schmidt, “Evaluation of Rayleigh-Sommerfeld diffraction formula for PML solutions”, The 8th International Conference on Mathematical and Numerical Aspects of Waves (2007)
- [9] C. Deaconu et al., “Measurements and modeling of near-surface radio propagation in glacial ice and implications for neutrino experiments”, Phys. Rev. D, 98, 043010 (2018)
- [10] R. G. Keys, “Cubic Convolution Interpolation for Digital Image Processing”, IEEE Trans. Acoust. 29, 1153–1160 (1981)
- [11] RNO-g Collaboration, Shower library, [https://rnog-data.zeuthen.desy.de/shower\\_library/](https://rnog-data.zeuthen.desy.de/shower_library/) (visited on 20/06/2023)
- [12] J. Alvarez-Muñiz, P. M. Hansen, A. Romero-Wolf, E. Zas, “Askaryan radiation from neutrino-induced showers in ice”, Phys. Rev. D 101, 083005 (2020)
- [13] J. Alvarez-Muñiz, W. R. Carvalho, Jr., M. Tueros, E. Zas, “Coherent Cherenkov radio pulses from hadronic showers up to EeV energies”, Astropart. Phys. 35, 287 (2012)